energies

MDPI

Article

Greenhouse Gas Reduction Effect of Solar Energy Systems Applicable to High-Rise Apartment Housing Structures in South Korea

Chang-Hyun Park [1], Yu-Jin Ko [1], Jong-Hyun Kim [2,*] and Hiki Hong [3,*]

[1] Department of Mechanical Engineering, Graduate School of KyungHee University, Yongin 17104, Korea; pli00001@naver.com (C.-H.P.); dbwlsrhdl@khu.ac.kr (Y.-J.K.)
[2] Department of Research Development, GENONE Energy, Anyang 14056, Korea
[3] Department of Mechanical Engineering, KyungHee University, Yongin 17104, Korea
* Correspondence: hyuns16@naver.com (J.-H.K.); hhong@khu.ac.kr (H.H.)

Received: 28 April 2020; Accepted: 16 May 2020; Published: 19 May 2020

Abstract: In South Korea, we are aiming for net zero energy use apartment home structures. Since the apartment structure in South Korea is generally a high-rise of 10 or more floors, the types of renewable energy applicable are limited to photovoltaic (PV) panels, solar collectors installed on the wall, or a photovoltaic thermal (PVT) hybrid panel combining both. In this study, the effect of PV, ST (Solar Thermal), and PVT systems on greenhouse gas reduction was analyzed using TRNSYS18. All three systems showed maximum CO_2 reductions at 35° facing south. PV, ST, and PVT showed CO_2 reductions of 67.4, 114.6, and 144.7 kg_CO_2/m^2·year, respectively. Compared to those values, when installed on a wall (slope of 90°), CO_2 reduction is about 35–40% less and about 20% less at a slope of 75°. ST and PVT installed on the vertical wall have a greater greenhouse gas reduction effect than the PV installed at the optimal slope of 35°. Since the CO_2 reduction difference among SW, SE, and azimuthal S is within 10%, ST and PVT are recommended for installation on high-rise apartment structure walls or balconies with the azimuthal angle of ±45° with respect to south.

Keywords: solar thermal system; photovoltaic; photovoltaic thermal; CO_2 reduction; energy production; TRNSYS18; high-rise apartment

1. Introduction

In response to the Paris Climate Change Accord for reducing greenhouse gases, South Korea has announced a strategy to expand its new 2030 energy industry [1]. In the energy construction field, standards for reducing greenhouse gases are being strengthened. In particular, Zero Energy Building is to become mandatory for new buildings from 2025 with plans to start in the public sector (2020) and expand to the private sector (2025). Hence, it is essential to introduce renewable energy along with high factor insulation, high performance windows, and heat recovery ventilation systems.

According to South Korea's national indicator system, the total number of households in the residential sector in 2018 was 19,979,000, of which about 9,550,000 were apartments. A large-scale refurbishment of ≥30-year-old apartment structures has recently been pursued, especially in the Seoul metropolitan area. According to Seoul ordinance, 14% or more of the expected energy consumption per total area of 100,000 m^2 must be covered by renewable energy sources. South Korean apartments are mostly high-rise structures with more than 10 floors, and the only renewable energy devices that can be applied to high-rise buildings are PV panels or solar collectors installed on walls or balconies [2,3].

PV systems have experienced price reductions and improvements in efficiency through continuous research and development of modules [2]. Moreover, due to solar PV expansion policies in many

countries and even the attainment of grid-parity in some countries, sustained growth is anticipated in the outdoor PV and building Integrated Photovoltaic (BIPV) markets [4–6]. For solar thermal systems, since 2000, attempts have been made mainly in Europe to develop a building-integrated solar collector that can be used as a building exterior material such as a BIPV module [7–9]. Facade-integrated solar collectors in particular have been used in houses in places such as Austria and Germany since the late 1990s [10,11]. Recently, in China, examples of one or two solar collectors on the walls or balconies of apartment houses have become common [12].

The growth of PV supply among renewable energy materials is remarkable both domestically and overseas [13,14]. In South Korea, PV is more widely used for power generation in parking lots and on factory roofs rather than for residential building consumption [15,16]. There are social problems such as some environmental destruction and ESS (Energy Storage System) fires when PV panels are installed in forests and at reservoirs, but it is certain that this is an advantageous method that can send produced energy over long distances. Solar thermal systems, on the other hand, are at a disadvantage for long-distance transportation, and they are more advantageously installed in or near buildings [16]. In general, solar thermal systems are installed on a building rooftop and are widely used for hot water and heating [17–19]. Overseas, BIST (Building Integrated Solar Thermal), which can be installed more flexibly, is being applied as a pilot project [4,20].

PV systems on apartment structures, which account for most building energy consumption, are multiplying in some municipalities, including Seoul. Solar thermal systems have been installed on the roofs of apartment houses and are used as a common heat source but their contribution is insignificant. For greenhouse gas reduction, it is time for more active application to apartment structures, along with redevelopment plans for existing apartments.

In this study, we calculated energy production and CO_2 reduction by slope and azimuth when a solar thermal collector, a PV panel, and a PVT hybrid system combining both were installed on a rooftop or outer wall in a South Korean apartment structure [21]. Through this, objective data can be generated to understand and quantify how much greenhouse gas reduction is achieved when the system is introduced in a limited area.

2. Simulation Method and System Modeling

Forms of renewable energy applicable to urban houses, especially high-rise residential structures, are very restricted. With the technology commercialized to date, solar energy is the only relevant solution. The rooftop or roof can be used on the top floor of detached buildings or high-rise apartments, but other households are compelled to use exterior walls. Despite their different uses, both PV and ST systems have become widespread, and PVT hybrid system combining these two has also reached the stage of commercialization [22,23]. Although direct comparison is not easy, we simulated systems consisting of products whose performance and price are the average in South Korea.

In this study, a simulation was performed using TRNSYS18 [24]. This software has been developed for unsteady state simulation of solar energy systems and has been upgraded for about 40 years, and so has been verified for dynamic analysis of ST and PV systems. To simulate with TRNSYS18, set values for the components that make up the actual system must be secured. Since it is not possible to cover all systems in South Korea, the solar thermal collectors and PV and PVT panels of E-MAX System Co., Ltd. which has general performance were simulated. The weather data used for the simulation was TMY2 Seoul, which is in the TRNSYS18 internal library, and the simulation interval was 0.1 h, totaling to 8760 h (one year).

Since the object of this study is solar energy applied to high-rise apartments, installation is restricted. As is well known, solar energy reaches its maximum production of the year when the slope is similar to the local latitude. When installed on the rooftop, the slope is typically low, but installation on the middle floors of the high rise structure is restricted to walls and balconies where panels can be installed vertically or slightly inclined. Slopes were therefore set to 20°, 35°, 75°, and 90°. Southern orientation of solar components is preferred in South Korea, which is located in the northern

hemisphere, but, due to the arrangement of apartments, many are facing west or east. For that reason, we included W, SW, S, SE, and E orientations to see the effects.

In the simulation, the ST system was used for a domestic hot water supply with a heat collection area of 4.18 m^2. The main components of the system are a flat-plate collector (Type1b) and a heat storage tank (Type60d, 200 L) with a built-in heat exchange coil. The performance of the ST system varies depending on the heat storage tank and the control method regardless of the collector, and, in a previous study [25], the performance of the system shown in Figure 1 was compared through simulations under various conditions. The most basic method is a heat exchange coil arranged only in the lower part of the heat storage tank and a constant flow rate. Contrary to this lower installation of heat exchange coil, our previous studies showed that the upper and side heating of the storage tank is more effective for higher stratification performance [26], as upper heating increases the temperature difference between the top and bottom of the storage tank. In such system, when the solar radiation condition is not strong, it can be seen that operating only the bottom coil or reducing the flow rate improves the solar energy collection efficiency by about 7%. In this study, the simulation was performed with this improved method with lower and upper heating heat storage tank and three-stage flowrate. Table 1 summarizes the specifications of the solar collector, heat storage tank, and pump applied to the simulation.

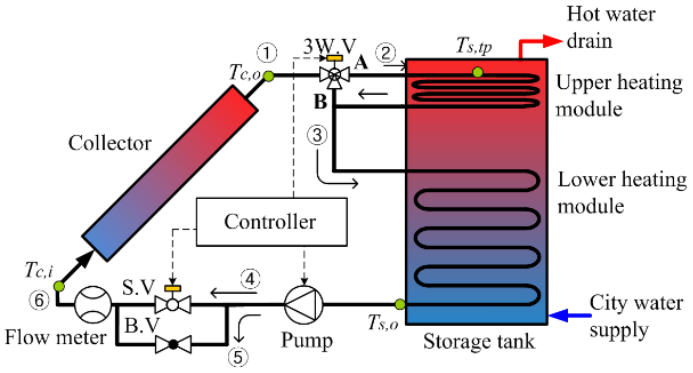

Figure 1. Schematic experimental set-up of solar combi-system. 3W.V, three-way valve; S.V, solenoid valve; B.V, bypass valve.

The load pattern and quantity greatly affect the performance of the solar water heater. When the load increases during the daytime, the temperature of the heat storage tank decreases, which leads to an improvement in solar energy collection efficiency. Daily hot water load of 150 L/day, the temperature of 60 °C, and the daily load of Cardinale et al. [27] in Figure 2 were applied. This is a typical usage pattern in a general household, and peak usage is concentrated in the morning and evening. The city water temperature is based on the monthly average value of the temperature at 1.5 m underground as provided by the South Korea Meteorological Administration and is summarized in Table 2.

Simulations for PV systems are relatively simple. Electricity was assumed to be connected to a grid and sent to a power company. A PV component (Type 194b) with an inverter was used. This component is appropriate for modeling the electrical performance of monocrystalline, polycrystalline, and thin film photovoltaic panels. Two modules in series with the same area (2.09 m^2) as the ST system were set. The performance data of the inverter were based on the default values built in TRNRSYS18, and Table 3 shows the important specifications required for the simulation.

Table 1. Specification of the solar thermal system.

Component	Category		Unit	Value
Collector	Area (Gross)		m^2	2.09
	Fluid heat capacity		kJ/kg·K	3.7
	Tested flow rate		kg/s·m^2	0.01835
	Intercept efficiency		-	0.6997
	Efficiency slope		W/m^2·K	3.6964
	Efficiency curvature		W/m^2·K^2	0.0104
Storage tank	Volume		L	200
	Height		m	1.1
	Material of heat exchanger		-	STS 304
	Upper heat exchanger (smooth tube)	Diameter × Length	m	15.8Φ × 5
		Height (Inlet, Outlet)	m	0.962 0.881
	Lower heat exchanger (smooth tube)	Diameter × Length	m	15.8Φ × 7
		Height (Inlet, Outlet)	m	0.175 0.067
Pump	Maximum flow rate		kg/s	0.073
	Maximum power		W	16.7

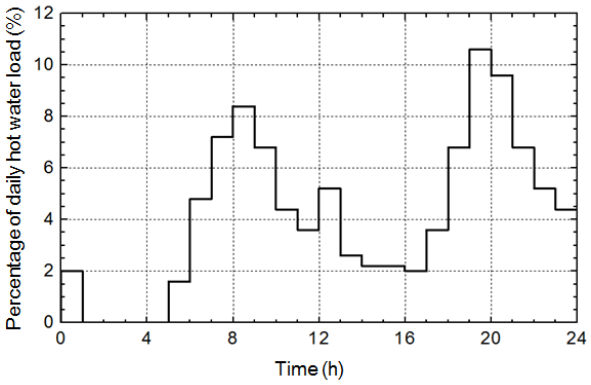

Figure 2. Daily load pattern (Cardinale et al. [27]).

Table 2. Average ground temperature in Seoul.

Category	Jan.	Feb.	Mar.	Apr.	May	Jun.	Jul.	Aug.	Sep.	Oct.	Nov.	Dec.
Temp (°C)	8.0	6.1	6.4	9.4	13.4	17.2	20.9	23.4	23.2	20.7	16.6	11.7

Figure 3 show a schematic diagram of the PVT system. The solar water heater is the same as Figure 1, and the relatively low water temperature is augmented through the auxiliary heater. The electricity produced was connected to the grid in the same way as PV. The configuration of the simulation is the same as that of the ST system except for the PVT component (Type 50d) and the inverter (Type 48b). Type 50d models a combined photovoltaic and thermal (PVT) solar collector by adding a PV module to the standard flat-plate collector. It is available in the default TRNSYS library, can be used with glazed and unglazed modules, and is the most widely used PVT Type. In the case of Type 48b (Inverter), if the battery is fully charged or needs only a taper charge, excess power is either dumped or not collected by turning off parts of the source. The inverter converts the DC power to AC and sends it to the load and/or feeds it back to the utility. For fair comparison, the heat storage tank,

load pattern, and control logic were all set identically. Inverter efficiency was set to 78%, similar to the default value built into the Type 194b used for the PV system. Figure 4 shows the configuration of the TRNSYS18 simulation of the PVT system, and Table 4 shows the specifications of the solar collector at the bottom of the PVT. The PV module of PVT is the same as the on in Table 3.

Table 3. Specification of the photovoltaic system (STC: 25 °C, 1 kW/m^2, Spectrum AM 1.5).

Category	Unit	Value
Module size	m^2	2.09
Open circuit voltage (V_{oc})	V	48.8
Short circuit current (I_{sc})	A	8.77
Maximum power (P_{max})	W	332.6
Voltage at maximum power (V_{mpp})	V	39.6
Current at maximum power (I_{mpp})	A	8.41
Fill factor	%	77.7
Module efficiency(η_C)	%	15.9
Number of cells	ea	72
Cell size	cm^2	242.7

Annual average horizontal solar radiation in South Korea: 4215 MJ/m^2 [28].

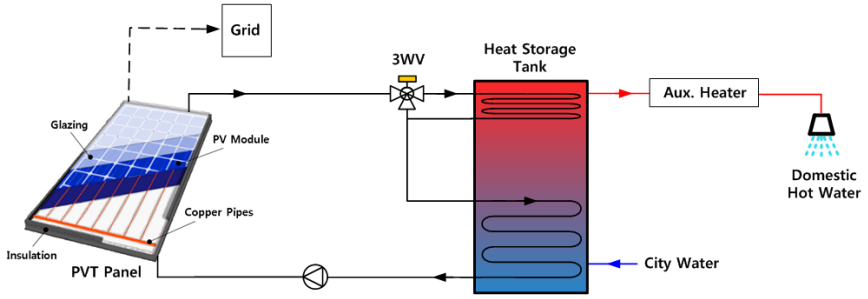

Figure 3. Schematic diagram of the PVT system.

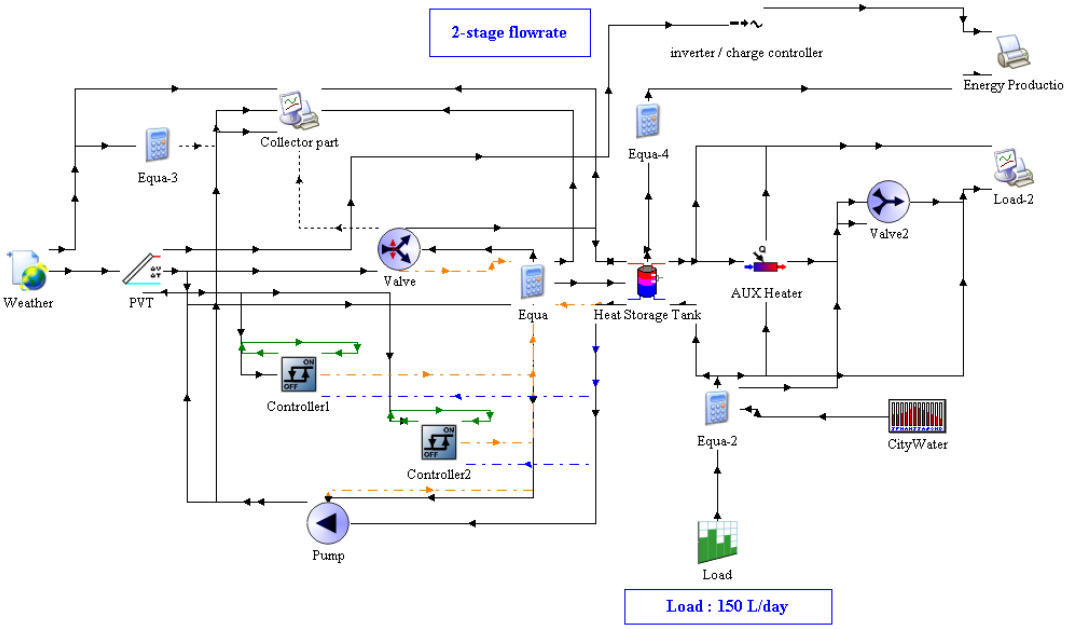

Figure 4. Composition of the PVT system TRNSYS18 simulation.

Table 4. Specification of the PVT system.

Collector	Type	Flat Plate Solar Collector				
	Size	1042 mm × 2002 mm × 58 mm				
	Area	Gross Area: 2.09 m^2, Transmission Area: 1.92 m^2				
	Tested flow rate	0.0385 kg/s				
	Intercept efficiency	0.5299				
	Efficiency slope	4.5752 $W/m^2 \cdot K$				
	Efficiency curvature	0.0206 $W/m^2 \cdot K^2$				
	Absorber plate	Material: A.L Plate, Titanium coated aluminum absorber Size : 985 mm × 1948 mm × 0.3 mm				
		Coating	Titanium coating			
		Absorptivity	95.1%			
		Reflectance	3.7%			
	Tube	Material: Copper Size : Diameter Φ12.7 mm, Thickness 0.89 mm, Length 23231 mm				
	Operating fluid	15% Propylene glycol				
Insulator		Material	Thickness (mm)	Density (kg/m^3)	Heat-resisting Temperature (°C)	Thermal Conductivity (W/m·K)
	Side	EPDM	10	45	409	0.033
	Bottom	EPDM	20	45	409	0.033

The heat and electricity produced by the PVT module were analyzed using the mathematical algorithm analysis method of TRNSYS 18 Mathematical

$$Q_{PVT} = A \times F_r \times (S - U_L(T_i - T_a)) \quad (1)$$

Equation (1) is the same as general solar collector formula. The electricity production rate (P_{PVT}) and photovoltaic cell efficiency (η_{PVT}) were calculated using Equations (2) and (3).

$$P_{PVT} = (\tau\sigma)_n IAM \times G_t \times A \times \eta_{PVT} \quad (2)$$

$$\eta_{PVT} = \eta_c \times X_t \times X_r \quad (3)$$

As the temperature of the panel rises, the temperature function X_t decreases, and electricity production decreases. Annual thermal efficiency ($\eta_{th,\ year}$), electrical efficiency ($\eta_{el,year}$), and solar fraction (f_{year}) are as follows.

$$\eta_{th,\ year} = \frac{\sum Q_{PVT}}{\sum G_t} \quad (4)$$

$$\eta_{el,year} = \frac{\sum P_{PVT}}{\sum G_t} \quad (5)$$

$$f_{year} = \frac{\sum Q_{DHW} - \sum Q_{AUX}}{\sum Q_{DHW}} \quad (6)$$

3. Experimental Results and Discussion

Under the conditions described previously, simulations for PV, ST, and PVT were performed at different slopes (20°, 35°, 75°, and 90°) and azimuthal angles (W, SW, S, SE, and E). From this, we calculated the amount of heat generated by each system, electricity produced, and associated reduction in CO_2 production.

3.1. CO_2 Calculation Method

The amount of CO_2 reduced by use of renewable energy can be calculated by figuring the amount of CO_2 generated when the same amount of heat or electricity is produced on a fossil fuel basis. Since the amount of CO_2 generated depends on the type of fuel, it is reasonable to choose the one that is most often used in apartments. For thermal energy, LNG (Liquefied Natural Gas), which accounts for 71% of heating in the housing sector in South Korea (90% of boiler efficiency, low heating value applied), was used as a reference [15]. In the case of electrical energy, there is an emission factor announced according to the composition of fuel used for power generation by country, and the carbon emission factor of South Korea is 0.1319 kg_C/kWh [29]. This value was applied to calculate the amount of greenhouse gas reduction due to electricity produced by PV. Calories and carbon emissions were calculated based on the data shown in Table 5.

Table 5. The conversion standard of energy units and IPCC carbon factor [16].

Category	Unit	Upper			Lower			Carbon Emission Factor	
		MJ	kcal	$\times 10^{-3}$ toe	MJ	kcal	$\times 10^{-3}$ toe	kg_C/GJ	ton_C/toe
Crude oil	kg	44.9	10,730	1.073	42.2	10,080	1.008	20.00	0.829
Gasoline	L	32.6	7780	0.778	30.3	7230	0.723	18.90	0.783
Kerosene oil	L	36.8	8790	0.879	34.3	8200	0.820	19.60	0.812
Diesel oil	L	37.7	9010	0.901	35.3	8420	0.842	20.20	0.837
Natural gas (LNG)	kg	54.6	13,040	1.304	49.3	11,780	1.178	17.20	0.630
City gas (LNG)	Nm^3	43.6	10,430	1.043	39.4	9420	0.942	15.30	0.637
City gas (LPG)	Nm^3	62.8	15,000	1.500	57.7	13,780	1.378	17.20	0.713
Electricity (generation)	kWh	8.8	2110	0.211	8.8	2110	0.211	0.1319 kg_C/kWh	
Electricity (consumption)	kWh	9.6	2300	0.230	9.6	2300	0.230	-	

LNG CO_2 emission calculation:

- Ton of oil equivalent (toe) = LNG Conversion (Nm^3) × LNG Lower Heating Value (toe/Nm^3)
- C emission (ton_C) = Ton of oil equivalent (toe) × LNG Carbon emission factor (ton_C/toe)
- CO_2 emission (ton_CO_2) = (CO_2 (Molar mass 44)/C (Molar mass 12)) × C emission (ton_C)
- Example) 200 MJ energy production in Jan. when slope is 45°. Boiler efficiency 90%, City gas (LNG) LHV Conversion value is 5.64 Nm^3
- Ton of oil equivalent (toe): 5.64 Nm^3 × 0.942 × 10^{-3} toe/Nm^3 = 5.31 × 10^{-3} toe
- C emission: 5.31 × 10^{-3} toe × 0.637 ton_C/toe = 3.38 × 10^{-3} ton_C
- CO_2 emission: (44/12) × 3.38×10^{-3} ton_C = 12.39 × 10^{-3} ton_CO_2

Electrical energy CO_2 emission calculation:

- Carbon (C) emission (kg_C) = Electrical energy production (kWh) × Carbon emission factor of electrical energy (kg_C/kWh)
- Carbon dioxide (CO_2) emission (kg_CO_2) = (CO_2 (Molar mass 44)/C (Molar mass 12)) × Carbon emission (kg_C)
- Example) 10 kWh energy production in Jan. when slope is 45°.
- C emission: 10 kWh × 0.1319 kg_C/kWh = 1.319 kg_C → 1.4×10^{-3} ton_C
- CO_2 emission: (44/12) × 1.319 kg_C = 4.84 kg_CO_2 → 4.84×10^{-3} ton_CO_2

3.2. Energy Production and CO_2 Reduction by Slope

Table 6 shows the annual energy production and CO_2 reduction as a result of simulating with the azimuth fixed to the south and at the slope of 20°, 35°, 75°, and 90°.

Table 6. Energy production and CO_2 reductions of the PV, ST, and PVT systems according to slopes.

Category		20°	35°	75°	90°
PV	kWh/m^2	137.4	139.4	111.9	90.9
	kg_CO_2/m^2	66.4	67.4	54.1	44.0
	Decreasing rate (%)	−1.5	0.0	−19.7	−34.7
ST	MJ/m^2	1756.1	1846.6	1427.8	1087.6
	kg_CO_2/m^2	109.0	114.6	88.6	67.5
	Decreasing rate (%)	−4.9	0.0	−22.7	−41.1
PVT	kWh/m^2	170.9	173.4	136.9	107.9
	MJ/m^2	949.9	980.5	751.3	563.6
	kg_CO_2/m^2	141.6	144.7	112.8	87.2
	Decreasing rate (%)	−2.1	0.0	−22.0	−39.8

PV, photovoltaic; ST, solar thermal; PVT, photovoltaic thermal.

As expected, PV, ST, and PVT all showed the highest energy production and CO_2 reduction at a slope of 35°. The annual solar radiation at 35° slope is 4.90 GJ/m^2 (1.36 MWh/m^2), and CO_2 reduction is PV 67.4 kg_CO_2/m^2 (Q_{el} = 139.4 kWh/m^2, $\eta_{el,\ year}$ = 10.3%), ST 114.6 kg_CO_2/m^2 (Q_{th} = 1846.6 MJ/m^2, $\eta_{th,\ year}$ = 37.8%), PVT 144.7 kg_CO_2/m^2 (Q_{th} = 980.5 MJ/m^2, Q_{el} = 173.4 kWh/m^2).

The electrical and solar energy collection efficiencies calculated from Equations (4) and (5) are smaller than the ones commonly known because the total time for the system to operate and produce energy is not very long, and the amount of solar radiation projected at other times is only included in the denominator of Equations (4) and (5).

At the slope of 90° installed on the wall, the CO_2 reduction was the smallest, and the values of PV, ST, and PVT were, respectively, 34.7%, 41.1%, and 39.8% lower than at the slope of 35°. At a slope of 75°, CO_2 reduction is reduced by about 20%. If only installation is possible, 75° slope is preferable to 90°, which is in close contact with a vertical wall.

Figure 5a shows the results of comparing the electricity production of PV and PVT systems according to tilt angle. Overall, PVT showed about 1.2 times greater production than PV, regardless of the slope. As shown in Equation (3), as the temperature increases, the efficiency modifier X_t decreases, the efficiency decreases, and consequently electricity production decreases. In the case of PVT, the heat medium lowers the temperature of the PV, so electricity production increases. In Reference [30], PV and PVT efficiency were compared through experiments. Similar to the results of this paper, the electricity production of PV and PVT systems during the day were calculated as 1030 and 1135 Wh, respectively showing that PVT is about 1.1 times greater.

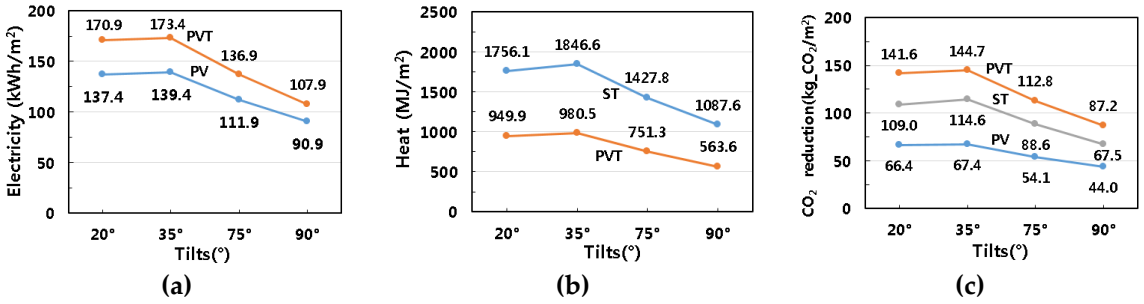

Figure 5. Energy production and CO_2 reduction according to the slope: (**a**) energy production of PV and PVT; (**b**) energy production of ST and PVT; and (**c**) CO_2 reduction of PV, ST, and PVT.

Figure 5b compares the heat production of the ST and PVT systems. Overall, PVT heat production was half that of ST, regardless of tilt angle. When used separately, the solar collector receives solar radiation directly, which is immediately converted to heat. In the case of PVT system, however, heat production is reduced because solar radiation is indirectly collected using heat of the PV module in the upper part.

Figure 5c compares the amount of CO_2 reduction by PV, ST, and PVT systems. Since PVT can produce electricity and heat simultaneously, it showed about 2.1 times greater CO_2 reduction than PV. ST reduction was about 1.6 times greater than that of PV.

It is very interesting that the ST installed on a vertical wall has almost the same and PVT has 1.4 times larger greenhouse gas reduction effect than the PV installed at an optimal inclination of 35°. Since this fact is almost without regard for the azimuthal angle, which is discussed below, it can be concluded that, at any slope, the application of ST or PVT is advantageous for reducing CO_2 wherever hot water is used.

It should be noted that, due to the nature of the simulation, there is an error from the actual system operation. In the case of PV system, among the various causes of loss, the factor that has the greatest influence on performance is loss due to module temperature, inverter efficiency, and angle of incidence change, which is considered through simulation [31]. However, performance degradation due to aging or natural phenomena such as corrosion, breakage, and soiling is not considered. Especially, as shown in Ref. [32], when the concentration of the fine dust is severe, the amount of power generation decreases by about 17–25% due to the decrease in the amount of solar radiation in the atmosphere and the dust accumulated on the surface of the PV module. In the case of ST system, in a previous study, it was proved that the simulation showed thermal efficiency of 1.1% lower than the experiment.

3.3. Influence of Azimuth

Table 7 summarizes the annual PV, ST, and PVT system energy production and CO_2 reduction according to tilt and azimuth. The PV showed maximum values in the southern direction for all slopes, and showed similar results in the southeastern and southwestern directions, which differed little from the southern direction. ST and PVT show generally similar trends. The difference is small, but, for ST, when at slopes of 75° and 90°, heat production was highest when facing southwest.

Figure 6 shows the amount of CO_2 reduction by azimuth. In all systems, maximum CO_2 reduction was at the slope of 35° facing south. At all slopes, the CO_2 reduction is greatest in the direction of south (S), followed by southwest (SW), southeast (SE), west (W), and east (E). SW CO_2 reduction in ST is slightly less than south, but not significantly. SE generally shows a decrease rate of less than 10% from the south. SW was 0.8% and 3.4% higher than the south at ST slope of 75° and 90°, respectively, but at a negligible level. Note that it is generally better to set up facing west than east, especially for ST.

Table 7. Energy production and CO_2 reductions of the PV, ST, and PVT systems according to slopes and azimuths.

Category		Energy (PV: kWh/m^2, ST: MJ/m^2)								CO_2 Reduction (kg_CO_2/m^2)			
		20°		35°		75°		90°		20°	35°	75°	90°
		PV	ST	PV	ST	PV	ST	PV	ST				
PV	E	118.6		111.9		83.3		70.3		57.3	54.1	40.3	34.0
	SE	131.5		131.3		102.9		85.5		63.6	63.5	49.8	41.3
	S	137.4		139.4		111.9		90.9		66.4	67.4	54.1	44.0
	SW	132.7		133.0		105.8		88.1		64.2	64.3	51.2	42.6
	W	120.2		114.3		86.4		73.0		58.1	55.3	41.8	35.3
ST	E		1430.6		1377.2		942.6		701.9	88.8	85.4	58.5	43.5
	SE		1651.6		1698.8		1297.7		984.9	102.5	105.4	80.5	61.1
	S		1756.1		1846.6		1427.8		1087.6	109.0	114.6	88.6	67.5
	SW		1707.8		1793.8		1439.5		1125.5	106.0	111.3	89.3	69.8
	W		1506.7		1499.0		1108.7		863.2	93.5	93.0	68.8	53.6
PVT	E	144.0	788.0	130.2	734.6	81.7	461.1	62.4	338.0	118.5	108.5	68.1	51.1
	SE	162.3	897.2	159.4	900.9	118.2	655.0	93.1	488.6	134.2	133.0	97.8	75.3
	S	170.9	949.9	173.4	980.5	136.9	751.3	107.9	563.6	141.6	144.7	112.8	87.2
	SW	163.6	927.1	161.3	949.1	121.0	740.7	95.7	584.9	136.7	136.9	104.5	82.6
	W	145.7	830.9	132.6	804.8	84.9	568.0	65.4	444.6	122.0	114.0	76.3	59.2

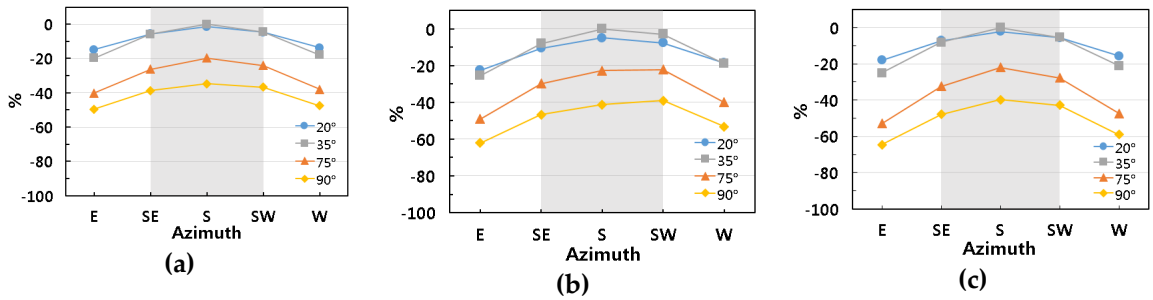

Figure 6. CO_2 reduction of the PV, ST, and PVT according to the slopes and the azimuths: (**a**) photovoltaic; (**b**) solar thermal; and (**c**) photovoltaic thermal.

In conclusion, the decreased rates of reduction at SW and SE are within 10% of the value resulting from the azimuth angle S. To maximize the reduction of CO_2 in high-rise apartments, ST and PVT are recommended for installation on walls or balconies with an azimuthal angle of S ± 45°. By exceeding this range, the amount of CO_2 reduction drops significantly at all slopes. The shaded area in Figure 6 is therefore recommended.

4. Conclusions

The only renewable energy that can be applied to high-rise apartment structures is a PV panel or solar collector installed on a wall or rooftop, or a PVT hybrid panel combining these two. We analyzed the greenhouse gas reduction effect when a 4.18 m^2 solar panel was applied. An annual simulation for PV, ST, and PVT systems was performed using TRNSYS18 with weather data from Seoul. The results are summarized as follows.

1. All three systems showed maximum CO_2 reduction values at 35° facing south, and PV, ST, and PVT showed reductions of 67.4, 114.6, and 144.7 kg_CO_2/m^2·year, respectively.
2. If installed on a vertical wall, the CO_2 reduction will decrease by about 35–40% compared to the maximum value, and the reduction will be about 20% less than maximum when installed at a slope of 75°. If it maintains harmony with the building, slightly inclined installation is better than vertical installation.
3. Regardless of the slope and azimuthal angle, ST has 1.6 times and PVT has 2.1 times greater CO_2 reduction than the PV which is most widely used in buildings.
4. It should be noted that ST (almost the same) and PVT (1.4 times) installed on vertical walls have a greater greenhouse gas reduction effect than PV installed at the optimal slope of 35°.
5. Since the decreased rate of CO_2 reduction when installed facing SW and SE is within 10% of the south facing reduction, ST and PVT are recommended for installation on walls or balconies with an azimuthal angle of S ± 45°.

Author Contributions: Conceptualization, H.H. and J.-H.K.; methodology, J.-H.K.; investigation, C.-H.P.; Data Curation, C.-H.P. and Y.-J.K.; writing—original draft preparation, H.H. and Y.-J.K.; and writing—review and editing, H.H. All authors have read and agreed to the published version of the manuscript.

Funding: This research received no external funding.

Conflicts of Interest: The authors declare no conflict of interest.

Nomenclature

Q_{PVT}	Thermal energy production rate of PVT (W)
Q_{el}	Electrical energy production rate of PV (kWh/m^2)
Q_{th}	Thermal energy production of PVT (MJ/m^2)
A	Area of PVT solar collector (m^2)
F_r	Collector heat removal factor
S	Solar radiation absorbed by a collector (W/m^2)
U_L	Collector overall heat loss coefficient (W/m^2·K)
T_i	PVT inlet temperature (°C)
T_a	PVT ambient temperature (°C)
P_{PVT}	Electric energy production rate of PVT (W)
$\tau\sigma$	Transmittance-absorptance product of solar collector
IAM	The incident angle modifier
G_t	The total radiation incident upon the collector surface (kW/m^2)
η_{pvt}	PV cell efficiency of PVT (%)
η_c	PV cell efficiency of PVT at reference condition (%)
X_t	Efficiency modifier (temperature), STC (1/K)
X_r	Efficiency modifier (incident radiation), STC (h·m^2/kJ)
$\eta_{th,\ year}$	Annual thermal efficiency of PV/PVT (%)
$\eta_{el,\ year}$	Annual electrical efficiency of ST/PVT (%)
f_{year}	Annual solar fraction
Q_{DHW}	Rate of thermal energy required for hot water (W)
Q_{AUX}	Rate of thermal energy used as auxiliary heater (W)

References

1. MOTIE. *To Respond to the New Climate System 「2030 New Industry of Energy Expansion Strategy」*; Ministry of Trade, Industry and Energy: Seoul, Korea, 2015.
2. Noh, J.Y.; Hwang, D.K. Solar Hot Water System and Photovoltaic System Performance Analysis in an Apartment. In Proceedings of the SAREK Summer Annual Conference, Yongpyong, Korea, 26–28 June 2013; pp. 339–342.
3. Kim, J.S.; Lee, E.J.; Hwang, J.H. A Study on Electric Capacity and CO_2 by the Roof Top PV System of the Industrial Building in Korea. *J. Korean Sol. Energy Soc.* **2010**, *30*, 131–136.

4. KEA. *Renewable Energy Trend Data*; Korea Energy Agency: Yongin, Korea, 2014.
5. De, R.K.; Ganguly, A. Energy, Exergy and Economic Analysis of a Solar Hybrid Power System Integrated Double-Effect Vapor Absorption System-Based Cold Storage. *Int. J. Air Cond. Ref.* **2019**, *26*, 1950018. [CrossRef]
6. Yang, H.S.; Park, H.S.; Yoon, H.K. A Comparative Analysis on the Generation Efficiencies of the Photovoltaic Systems and Building Integrated Photovoltaic Systems. *J. Arch. Inst. Korea Plan. Des.* **2013**, *29*, 37–44.
7. Hestnes, A.G. Building Integration of Energy Systems. *Sol. Energy* **1999**, *67*, 181–187. [CrossRef]
8. Yang, T.; Athienitis, A.K. Experimental Investigation of a Two-Inlet Air-Based Building Integrated Photovoltaic/Thermal (BIPV/T) System. *Appl. Energy* **2015**, *159*, 70–79. [CrossRef]
9. Motte, F.; Notton, G.; Christian, C.; Canaletti, J.-L. Design and Modelling of a New Patented Thermal Solar Collector with High Building Integration. *Appl. Energy* **2013**, *102*, 631–639. [CrossRef]
10. Yoon, J.H. The Latest Technology of Building Integrated Photovoltaic(BIPV) and Solar Thermal(BIST) Systems. *Constr. Technol. Rev. Ssangyong* **2011**, *59*, 4–9.
11. Leone, G.; Beccali, M. Use of Finite Element Models for Estimating Thermal Performance of Facade-Integrated Solar Thermal Collector. *Appl. Energy* **2016**, *171*, 392–404. [CrossRef]
12. Shi, J.; Su, W.; Zhu, M.; Chen, H.; Pan, Y.; Wan, S.; Wang, Y. Solar Water Heating System Integrated Design in High-Rise Apartment in China. *Energy Build.* **2013**, *58*, 19–26. [CrossRef]
13. Windholz, B.; Zauner, C.; Rennhofer, M.; Schranzhofer, H. Solar Thermal Energy Conversion and Photovoltaics in a Multifunctional Façade. In Proceedings of the CISBAT, Lausanne, Switzerland, 14–16 September 2011.
14. Luo, X.; Hou, Q.; Wang, Y.; Xin, D.; Gao, H.; Zhao, M.; Gu, Z. Experimental on a Novel Solar Energy Heating System for Residential Buildings in Cold Zone of China. *Procedia Eng.* **2017**, *205*, 3061–3066. [CrossRef]
15. KEEI. *2014 Energy Consumption Saurvey*; Korea Energy Economics Institute: Ulsan, Korea, 2015.
16. KEA. *New & Renewable Energy Supply Statistics 2014, 2015 ed.*; Korea Energy Agency: Yongin, Korea, 2015.
17. Yoon, J.H.; Sim, S.R.; Shin, U.C.; Kwak, H.Y. A Study on the Optimum Application Method of Solar Thermal System to reduce Thermal Load and Carbon Emission in Apartment Building. *J. Korean Sol. Energy Soc.* **2011**, *31*, 135–142. [CrossRef]
18. Shrivastava, R.; Kumar, V.; Untawale, S. Modeling and Simulation of Solar Water Heater: A TRNSYS Perspective. *Renew. Sustain. Energy Rev.* **2017**, *67*, 126–143. [CrossRef]
19. Valdiserri, P. Evaluation and control of thermal losses and solar fraction in a hot water solar system. *Int. J. Low Carbon Technol.* **2018**, *13*, 260–265. [CrossRef]
20. Nasruddin, M.I.; Lubis, A.; Satio, K.; Yabase, H.; Aisyah, N. Energy Analysis for the Solar Thermal Cooling System in Universitas Indonesia. *Int. J. Air Cond. Ref.* **2019**, *26*, 1950023.
21. Dubey, S.; Subiantoro, A. Numerical Study of Integrated Solar Photovoltaic Thermal Module with a Refrigeration System for Air-Conditioning and Hot Water Production under the Tropical Climate Conditions of Singapore. *Int. J. Air Cond. Ref.* **2018**, *26*, 1850021. [CrossRef]
22. Her, E.J.; Bae, S.; Kim, J.M.; Nam, Y. Feasibility Analysis based on Energy Simulation of PVT Hot Water System. *Korean J. Air Cond. Ref. Eng.* **2019**, *31*, 312–321.
23. Pressani, M.; Sommerfeldt, N.; Madani, H. Investigation of PV/Thermal Collector Models for Use with Ground Source Heat Pumps in Transient Simulations. In Proceedings of the EuroSun Conference, Palma de Mallorca, Spain, 19 August 2016.
24. Klein, S.A. *TRNSYS18 Base Manual*; KES Tech: Kocaeli, Turkey, 2019.
25. Kim, J.H.; Li, L.; Lee, U.J.; Hong, H. Performance Enhancement of Solar Thermal Storage Tank with Heat Exchange Coils (Part 2: Simulation). *Korean J. Air Cond. Ref. Eng.* **2016**, *28*, 361–366.
26. Son, H.S.; Kwon, J.W.; Lee, S.H.; Kim, C.; Hong, H. The effect of upper-heating system in solar water storage tank. *Int. J. Air Cond. Ref.* **2014**, *22*, 1450027. [CrossRef]
27. Cardinale, N.; Piccininni, F.; Stefanizzi, P. Economic Optimization of Low-Flow Solar Domestic Hot Water Plants. *J. Renew. Energy* **2003**, *28*, 1899–1914. [CrossRef]
28. Korea Meteorological Administration. Available online: https://www.weather.go.kr/weather/main.jsp (accessed on 12 May 2020).
29. KEC. *Guidelines for Local Government Greenhouse Gas Inventories*; Korea Environment Corporation: Sungnam, Korea, 2017.

30. Ozgoren, M.; Aksoy, M.; Bakir, C.; Dogan, S. Experimental Performance Investigation of Photovoltaic/Thermal (PV–T) System. In Proceedings of the EPJ Web of Conferences, Caen, France, 28–31 May 2013; EDP Sciences: Les Ulis, France, 2013; p. 01106.
31. Kwon, O.H.; Lee, K.S. Photovoltaic System Energy Performance Analysis Using Meteorological Monitoring Data. *J. Korean Sol. Energy Soc.* **2018**, *38*, 11–31.
32. Bergin, M.H.; Ghoroi, C.; Dixit, D.; Schauer, J.J.; Shindell, D.T. Large Reductions in Solar Energy Production Due to Dust and Particulate Air Pollution. *Environ. Sci. Technol. Lett.* **2017**, *4*, 339–344. [CrossRef]